**SOUTH COAST AIR QUALITY MANAGEMENT DISTRICT**

# Planetary Boundary Layer Height for Aircraft Emissions Inventory

## June 2025


**Deputy Executive Officer**
Planning, Rule Development, and Area Sources
Sarah Rees, Ph.D.

**Assistant Deputy Executive Officer**
Planning, Rule Development, and Area Sources
Ian MacMillan

**Planning and Rules Manager**
Planning, Rule Development, and Area Sources
Sang-Mi Lee, Ph.D.

Authors: Cui Ge, Ph.D. – Air Quality Specialist

Jonathan Liu, Ph.D. – Air Quality Specialist

Marc Carreras Sospedra, Ph.D. – Program Supervisor

# CONTENTS

# INTRODUCTION

Mixing height refers to the vertical extent of the atmosphere near the ground where pollutants, like smoke, are effectively mixed by turbulence. It is essentially the "lid" of the lower atmosphere, indicating how high pollutants can rise and disperse due to turbulent mixing. Mixing height is a critical parameter in calculating the aircraft emissions inventory. Emissions within the mixing height are included in the emissions inventory for State Implementation Plan (SIP), whereas emissions above the mixing height are excluded in SIP inventories or conformity budgets.[1] However, emissions above the mixed layer are still estimated and accounted for the regional photochemical modeling, although their impact on ground-level air quality is anticipated less significant than that of emissions within the mixing layer. The mixing height is estimated at every airport using planetary boundary layer (PBL) height. This report evaluates various datasets and methodologies to determine the PBL height and presents a recommendation from the South Coast Air Quality Management District (AQMD) for use in the revised aircraft emissions for the upcoming SIP, which addresses the 2024 annual PM2.5 National Ambient Air Quality Standard (NAAQS) of 9 $\mu g/m^3$.

The most common, gold-standard method of determining PBL height is measurement via radiosondes. Radiosondes measure key atmospheric data and are equipped by a weather balloon and then launched into the atmosphere twice a day (Seidel et al. 2010). There are no radiosondes sites in the Basin. However, one of the closest radiosonde sites is the Miramar (NKX) station, located 55 km south of the Basin's southern boundary. Data from this site is routinely used as an input for dispersion modeling for South Coast AQMD's permit applications[2], as well as in the agency's daily operational air quality forecast.

Other observational data sources used to calculate PBL height include LIDAR, ceilometer and a variety of remote sensing products that provide vertical profiles such as atmospheric temperature, pressure, moisture, wind, refractivity or backscatter (Seibert et al., 2000, Zhang et al., 2022, Kalmus et al., 2022, Natalia et al., 2024). However, each observational method comes with its own limitations.

Radiosondes have limited spatial coverage and observe data only twice per day, limiting inference on diurnal variation. LIDAR may struggle with PBL height detection in stable conditions (Zhang et al. 2022). Ceilometers are inexpensive and perform well under overcast conditions, but have limited spatial coverage, which can introduce errors when skies are heterogeneous and prevent the ceilometer from detecting a true cloud base (Australian Government Bureau of Meteorology, 2024). Furthermore, they correlate weakly with radiosondes during stable conditions and may fail to detect upper-level clouds under clear or sparsely clouded conditions (Zhang et al. 2022, Vagner et al., 2016). Finally, different retrieval algorithms—such as the cluster, gradient, and Haar wavelet methods—vary in their sensitivity

[1] Code of Federal Regulations, 2011, Title 40 § 93.153 (2011): 598-602. Available at https://www.ecfr.gov/current/title-40/part-93/section-93.153#p-93.153(c)(2)(xxii)

[2] https://www.aqmd.gov/home/air-quality/meteorological-data/data-for-aermod

to signal noise, with some struggling more than others during rain events or periods of strong wind (Caicedo et al., 2017).

In consideration of the limitations highlighted above, this report discusses PBL height as it is calculated using a set of modeling approaches and one novel source of data. Various approaches are detailed, concluding with a discussion of South Coast AQMD's final choice in PLB height calculation.

# DATA AND METHODOLOGY

## Data Included in this Study

This study analyzes various data sources that are an alternative to ceilometer and LIDAR-based observations. These include modeled estimates from a variety of sources that integrate meteorological measurements with numerical weather prediction, and PBL height derived from aircraft observations. Datasets that integrate meteorological measurements with numerical weather model predictions provide continuous, spatially extensive atmospheric data. This report analyzed three datasets under this option: Reanalysis v5 (ERA5) from the European Centre for Medium-Range Weather Forecasts (ECMWF), and the North American Regional Reanalysis (NARR) and the North American Mesoscale (NAM) analyses datasets from the National Centers for Environmental Prediction (NCEP). It is noted that the NAM analysis data includes the assimilation of satellite data, aircraft data and other sources. A second option is to use the reanalysis data to drive a high-resolution weather model of which prediction can inform PBL height. The NARR data was used to as initial and boundary values and for analysis nudging to simulate the Weather Research Forecast (WRF) model at 4 km × 4 km grid resolution. For comparison, PBL height is also computed using radiosonde observations from near the basin and local meteorological measurements to run the meteorological data preprocessor AERMET[3].

Another novel source of data for PBL height calculation is meteorology data from aircraft data. In the US, commercial aircraft upload automated weather reports in a system known as the Aircraft Communications Addressing and Reporting System (ACARS). These data include several key pieces of information necessary for PBL height calculations, including date and time, longitude and latitude coordinates, altitude, temperature, and wind speed and direction. Previous studies have evaluated the use of ACARS data for PBL height calculation, noting that ACARS records lower atmospheric data with high levels of temporal resolution (English et al. 2024). ACARS is present on all commercial flights; around busy airports, data at many altitudes are well-represented.

Table 1 summarizes the datasets analyzed in this report. The ERA5, NARR, NAM, and AERMET data represent the year 2021, while the NARR WRF data represent 2018. ACARS data were collected from the year 2023.

[3] https://www.epa.gov/scram/meteorological-processors-and-accessory-programs

**TABLE 1**
**THE SPATIAL AND TEMPORAL RESOLUTION OF VARIOUS DATA SETS USED TO EVALUATE PBL HEIGHT ESTIMATES**

| DATA | Temporal Resolution | Horizontal resolution | Vertical resolution | Year |
|---|---|---|---|---|
| ERA5 | hourly | 0.25° X 0.25° | 37 pressure levels | 2021 |
| NARR | 3 hourly | 32 km X 32 km | 30 pressure levels | 2021 |
| NAM | 6 hourly | 12 km X 12 km | 40 pressure levels | 2021 |
| NARR WRF | hourly | 4 km X 4 km | 30 pressure levels | 2018 |
| AERMET | hourly | Point | | 2021 |
| ACARS | hourly | Point | Point | 2023 |

## PBL Height from Numerical Weather Models

*Overview*

In addition to observational products like ceilometers and ACARS, PBL height can be estimated by numerical weather modeling. One option is the use of datasets that integrate meteorological measurements with numerical weather model predictions like ERA5, NARR, and NAM. A second option is to use the reanalysis data to drive a high-resolution weather model of which prediction can inform PBL height. In this study, the NARR data was used as initial and boundary values and for analysis nudging to simulate the WRF model, generating another set of PBLH estimates (NARR WRF).

Table 2 below provides a summary of the NARR WRF configuration used in this study. This NARR WRF configuration uses the Yonsei University (YSU) scheme, which defines the PBL top as the height where a critical bulk Richardson number becomes zero – based on the buoyancy profile. In this approach, the PBL top corresponds to the maximum entrainment layer, as opposed to the layer at which the diffusivity becomes zero (Hong et al. 2006). The year 2018 was selected for the NARR WRF data because it was the modeling year for the recent South Coast Air Basin Attainment Plan for the 2012 Annual PM2.5 Standard (PM2.5 Plan), [4] and its performance was thoroughly evaluated. More detailed information regarding the NARR WRF performance evaluation can be found in Appendix II of the PM2.5 Plan.

[4] South Coast Air Basin Attainment Plan for the 2012 Annual PM2.5 Standard. Available at: https://www.aqmd.gov/home/air-quality/air-quality-management-plans/other-state-implementation-plan-(sip)-revisions/2012-annual-pm2-5-plan

**TABLE 2**
**OVERVIEW OF NARR WRF CONFIGURATION**

| Numerical platform | WRF V4.4.2 |
|---|---|
| Number of domains | 3 nested domains |
| Nested domain setting | D01: 36 Km (83 x 83) |
| | D02: 12 Km (169 X 169) |
| | D03: 4 Km (163 X 115) |
| Vertical layers | 30 layers, the lowest layer is at ~ 20 m above ground level |
| Simulation length | 4 days with 24-hour spin-up |
| Initial and boundary values | NCEP NARR[1] Re-analysis (32 km X 32 km) |
| Sea surface temperature | GHRSST[2] |
| Boundary layer scheme | YSU[3] scheme |
| Land Surface model | Pleim-Xiu |
| Cumulus parameterization | Kain-Fritsch |
| Micro physics | WRF Single-Moment 3-class |
| Radiation | RRTM scheme for longwave, Dudhia scheme for shortwave |
| Four-dimensional data analysis | Analysis nudging with NWS surface and upper air measurements |

[1]NARR - North American Regional Reanalysis
[2]GHRSST - The Group for High Resolution Sea Surface Temperature (https://www.ghrsst.Org/)
[3]YSU - Yonsei University

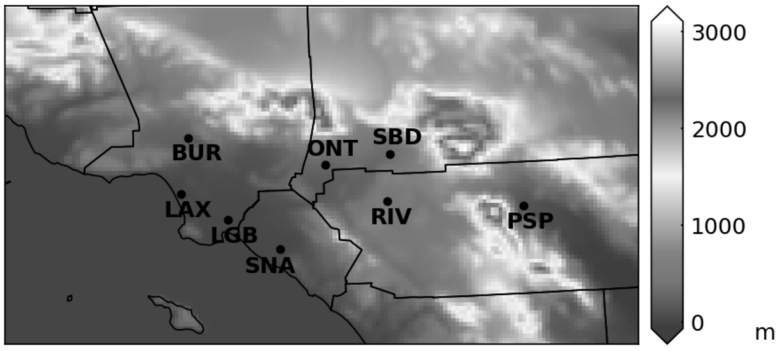


**FIGURE 1**
**TOPOGRAPHY IN THE BASIN AND MONITORING STATIONS. LOS ANGELES INTERNATIONAL AIRPORT (LAX), ONTARIO INTERNATIONAL AIRPORT (ONT), JOHN WAYNE AIRPORT (SNA), LONG BEACH AIRPORT (LBG), HOLLYWOOD BURBANK AIRPORT (BUR), SAN BERNARDINO INTERNATIONAL AIRPORT (SBD), PALM SPRINGS INTERNATIONAL AIRPORT (PSP), MARCH AIR FORCE RESERVE BASE (RIV)**

*NARR WRF Evaluation*

Figure 1 displays the locations of the major airports in the Basin. The performance of NARR WRF simulations for ONT is shown in Figure 2 through Figure 5. The model performance was evaluated for each month at airport stations in the model domain for January through December 2018. The observational data is collected from the National Weather Service (NWS) at major airports. For simplicity, only one summer month (July) and one winter month (January) for ONT station are shown. More NARR WRF modeling evaluations can be found in Appendix II of the PM2.5 Plan.[5]

Diurnal variations of temperature, humidity and surface wind were well represented by the NARR WRF simulations. Temperature and wind speed predictions were more accurate in the summer season than the winter months (Figure 2 – Figure 3). For example, the NARR WRF simulations for ONT station showed some underestimation of daily maximum temperatures during January of 2018. And the NARR WRF simulation showed better performance in predicting daily maximum temperatures in the summer. Both observational data and NARR WRF simulations at ONT station showed distinct diurnal variations in wind speed during the summer, with a strong sea breeze in the early afternoon. Daily maximum wind speeds were relatively consistent throughout July 2018, with much more variability observed during January 2018 (e.g., range of daily maximum wind speeds from ~2m/s to larger than 10 m/s during January from both measurements and simulations). The model performance in predicting the wind speed was significantly better for July 2018 compared to January 2018; R values for model-observation correlations were 0.79 in July 2018. The NARR WRF simulations yield water vapor mixing ratios comparable to observed values in both January and July at ONT station. The model-observation correlation coefficients are 0.87 in January 2018 and 0.74 in July 2018.

[5] South Coast Air Basin Attainment Plan for the 2012 Annual PM2.5 Standard. Available at: https://www.aqmd.gov/home/air-quality/air-quality-management-plans/other-state-implementation-plan-(sip)-revisions/2012-annual-pm2-5-plan

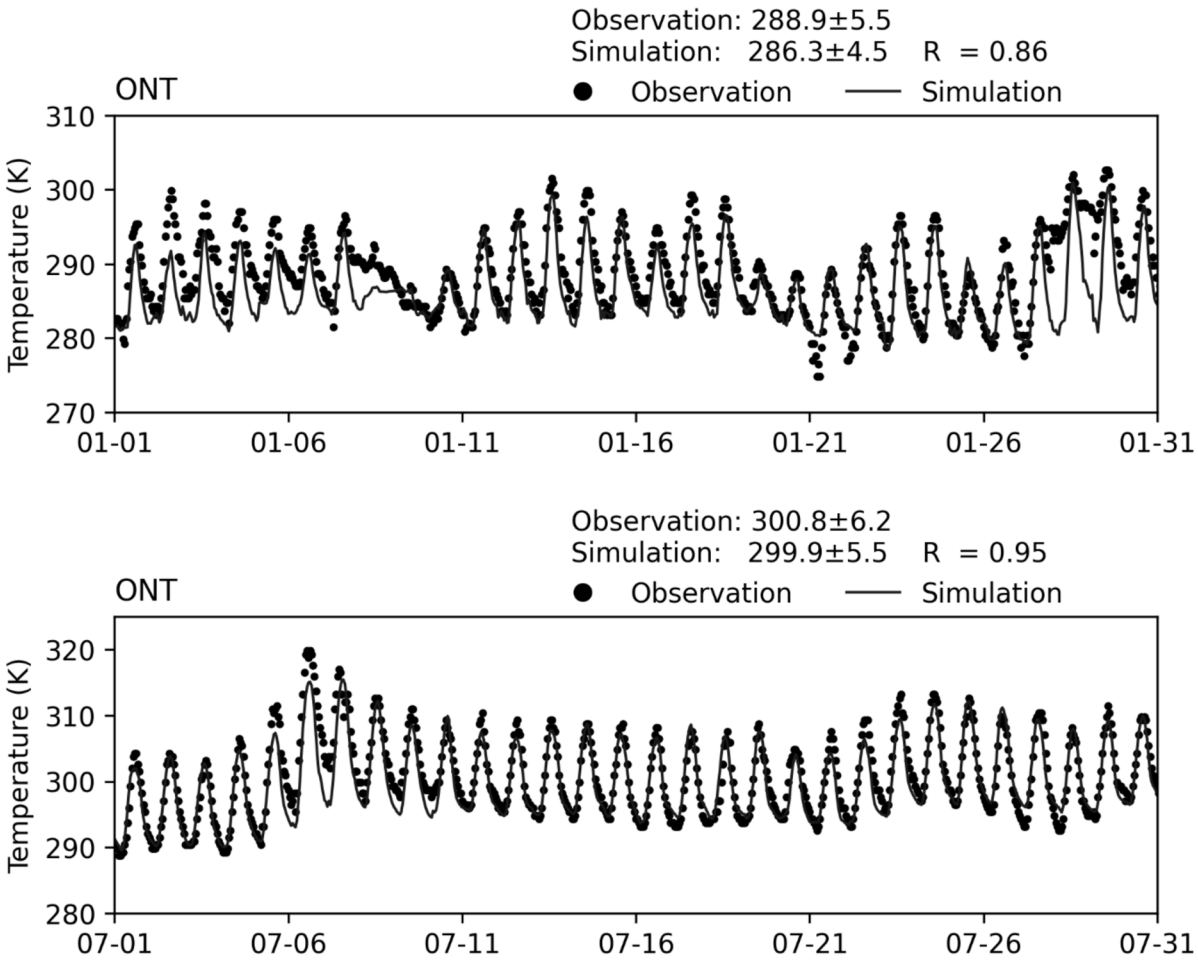


**FIGURE 2**
**TIME SERIES OF HOURLY TEMPERATURE FROM MEASUREMENT AND NARR WRF SIMULATIONS AT ONT STATION FOR JANUARY AND JULY OF 2018**

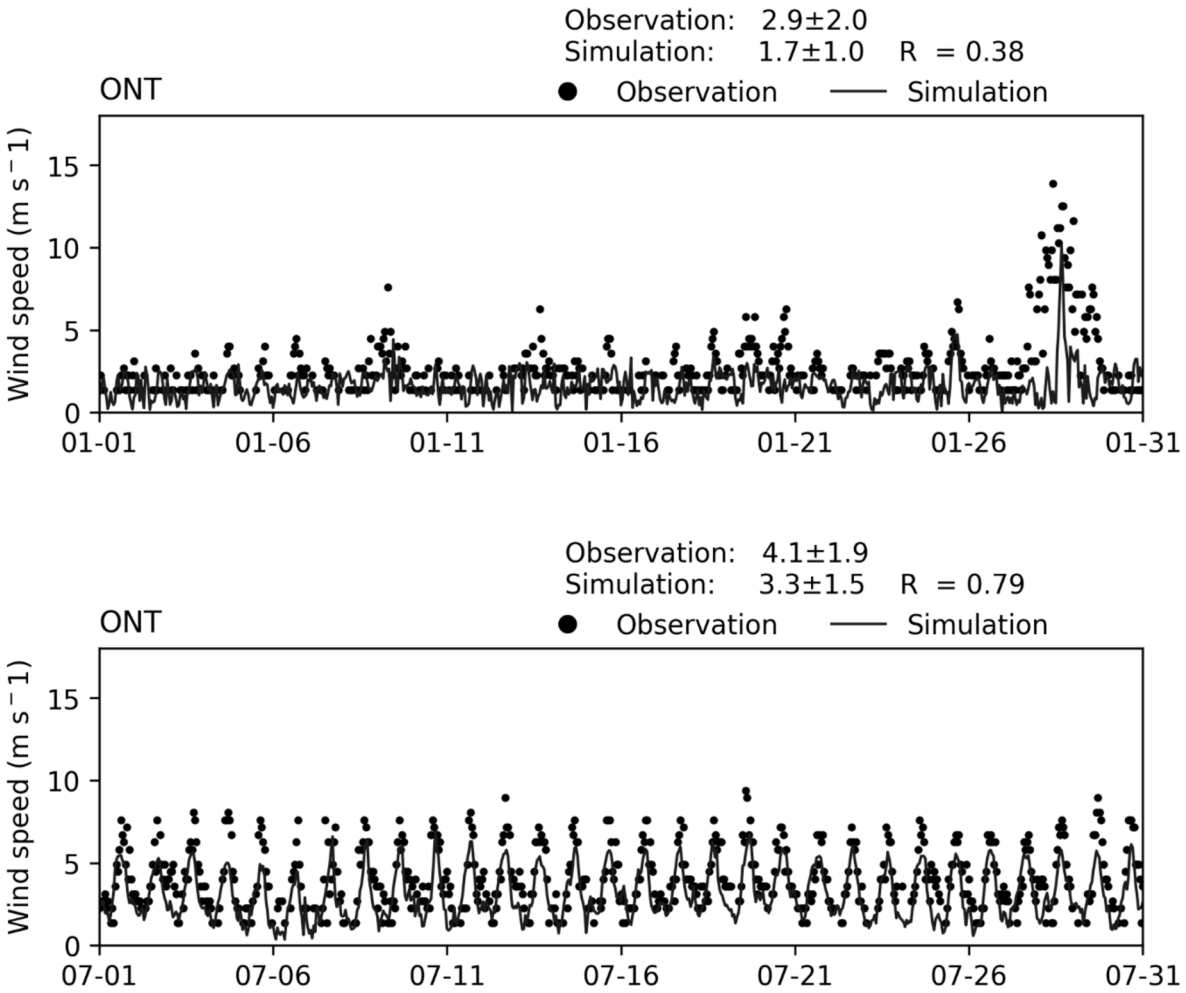


**FIGURE 3**
**TIME SERIES OF HOURLY WIND SPEED FROM MEASUREMENTS AND NARR WRF SIMULATIONS AT ONT STATION FOR JANUARY AND JULY OF 2018**

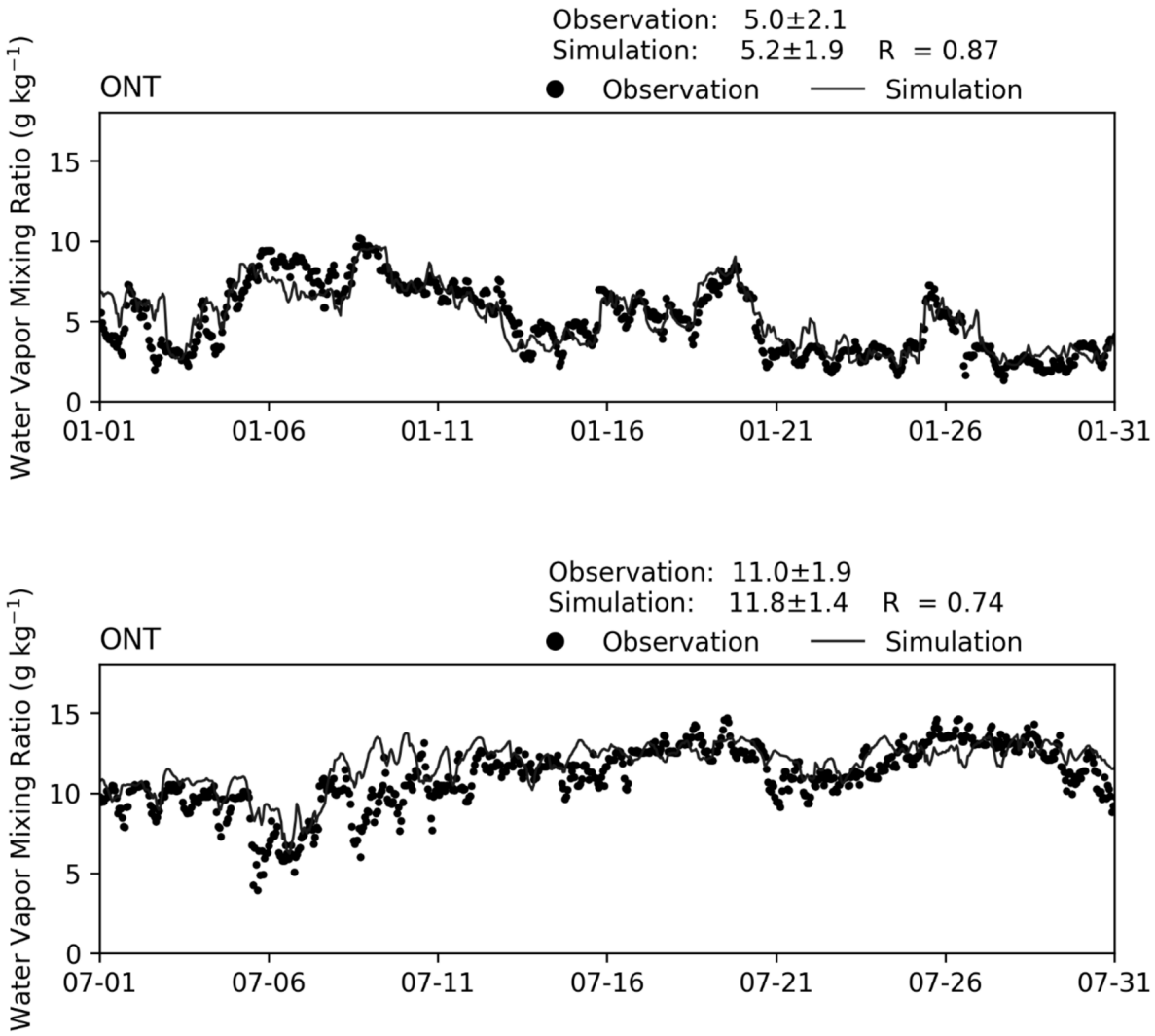


**FIGURE 4**
**TIME SERIES OF HOURLY WATER VAPOR MIXING RATIO FROM MEASUREMENTS AND NARR WRF SIMULATIONS AT ONT STATION FOR JANUARY AND JULY OF 2018**

The measured and NARR WRF simulated wind rose at ONT station for 1-year period of January – December 2018 are shown in Figure 5. The NARR WRF simulation successfully reproduces the dominant wind direction, with both the model and observations indicating prevailing south-westerly winds. However, the model tends to underestimate wind speeds compared to observations at ONT station.

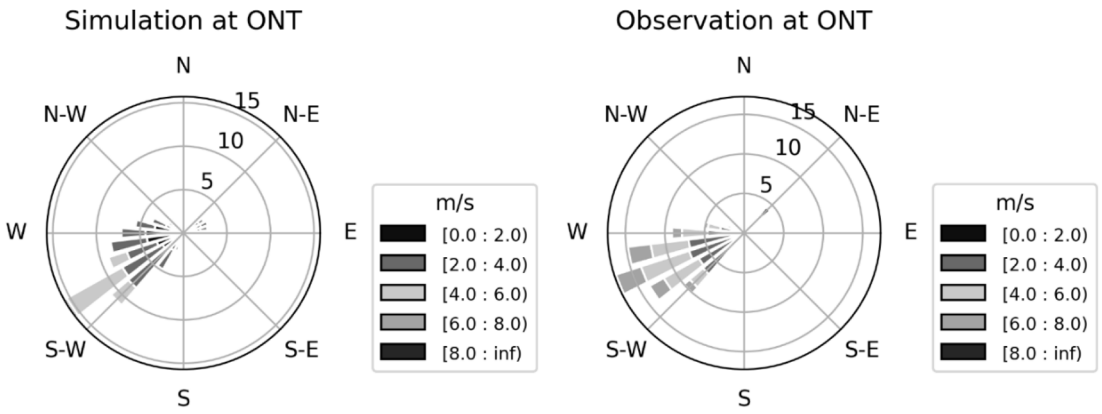


**FIGURE 5**
**WIND ROSE FROM MEASUREMENT AND NARR WRF SIMULATION AT ONT STATION IN 2018**

## PBL Height from AERMET with Radiosonde Data

As stated above, data from the NKX site are routinely used as an input for dispersion modeling for South Coast AQMD's permit applications[6], as well as in the agency's daily operational air quality forecast. The meteorological data preprocessor AERMET[7] can use the upper-air data from Miramar, along with surface meteorological observations, to estimate hourly PBL heights. Surface data from South Coast AQMD monitoring stations and Automated Surface Observing System (ASOS) stations within the AQMD's jurisdiction were collected for the year of 2021 and processed using U.S. EPA's AERMET Version 22112.

AERMET calculates the PBL height separately for convective (daytime) and stable (nighttime) atmospheric conditions using surface and upper air meteorological data. During convective conditions, AERMET employs a surface energy balance approach to estimate the surface sensible heat flux, then iteratively solves for the friction velocity (u*) and Monin–Obukhov length (L). These parameters are used to compute the convective velocity scale, which, along with empirical relationships, determines both the convective mixing height and the mechanical mixing height. The final mixing height is set as the greater of these two values.

Under stable conditions, AERMET does not use the energy balance method; instead, it estimates u* using an assumed temperature scale based on cloud cover, then calculates L accordingly. The mixing height is then determined solely from mechanical turbulence, which is smoothed temporally to ensure consistency. This AERMET data is publicly available and is recommended for use in South Coast AQMD permit applications when more accurate in-situ data is not available. However, unlike the WRF model,

[6] https://www.aqmd.gov/home/air-quality/meteorological-data/data-for-aermod

[7] https://www.epa.gov/scram/meteorological-processors-and-accessory-programs

AERMET has limitations in accounting for spatial variability, terrain effects, or the influence of the ocean marine layer; AERMET only accounts for these factors to the degree reflected in point-based measurement data used as input data.

In this study, AERMET-derived PBL heights are used for inland locations such as ONT and RIV, which are not directly influenced by land-sea contrasts or arid climate conditions that are poorly represented by AERMET's micrometeorological assumptions. ONT and RIV are located 136 and 112 km away from the Miramar sounding station, respectively. At these sites, AERMET's PBL height estimates serve as observational references to evaluate whether results from other methods are within a realistic range.

## Aircraft Measurements

### *Overview*

ACARS data include several key pieces of information necessary for PBL height calculations, including date and time, longitude and latitude coordinates, altitude, temperature, and wind speed and direction. Previous studies have evaluated the use of ACARS data for PBL height calculation, noting that ACARS records lower atmospheric data with high levels of temporal resolution (English et al. 2024). ACARS is present on all commercial flights; around busy airports, data at many altitudes are well-represented near large airports.

### *Evaluation*

Evaluation of ACARS data in this report features methods that mirror those of previous studies (English et al. 2024, Dai et al. 2014). Data were sourced from NOAA's Meteorological Assimilation Data Ingest System (MADIS), which consolidates various aircraft-related meteorological data, including flight data from ACARS. Once ACARS data were downloaded, flights were restricted to a 12 km radius around the following airports in the South Coast Air Basin: LAX, ONT, SNA, LGB, BUR, SBD, PSP, and RIV. Additional ACARS data around the NKX radiosonde were downloaded to evaluate the accuracy of the flight data, using the NKX radiosonde as a gold standard. Additional evaluation metrics include data completeness, which tracks the number of observed data points compared to the expected number over 24 hours and over an entire month.

Flights were binned into intervals of 50 meters, and within each altitude bin, the average temperature, wind speed (circular average), and relative humidities were calculated as well as their rate of change per 50 meters. Based on previous literature, the following methods were used to calculate PBL height with observe data: (1) the temperature gradient method, which estimates PBL height by analyzing the potential temperature gradient and identifying its maximum point and (2) the Richardson number method, which provides an estimate of turbulence, was also identified as a useful technique for determining PBL height. The Richardson number $Ri$, an estimate of turbulence, is calculated with the following equation:

$$Ri(z) = \left(\frac{g}{\theta v(z)}\right) * \left(\frac{\frac{\partial \theta v}{\partial z}}{\left(\frac{\partial U}{\partial z}\right)^2 + \left(\frac{\partial V}{\partial z}\right)^2}\right)$$

Where:

- $g$ refers to gravitational acceleration (9.81 m/s^2)
- $\theta_v$ refers to potential temperature (K)
- $z$ refers to altitude (meters)
- $U, V$ refer to horizontal wind components

Under method (1), the PBL height is derived by observing the altitude where the average temperature experiences the largest increase. Under method (2), based on the literature we start with a threshold of 0.25. The PBL height is set to the point where the $Ri$ exceeds the threshold. If the $Ri$ does not exceed 0.25, then another cutoff of 0.15 is used. The maximum value of the two methods is used for the final PBL height.

*Evaluation results*

Comparisons between ACARS data and the radiosonde at the NKX monitoring site are shown in Figure 6 and Figure 7. Figure 6 depicts the distribution of altitudes reported by the radiosonde (left) and the flight data (right). The sources of these two datasets are fundamentally different. Radiosonde data comes from controlled launches, typically conducted twice per day at 00 and 12 GMT, while flight data consists of continuous observations made by airplanes throughout the day. These differences in data collection methods lead to distinct characteristics in the resulting information.

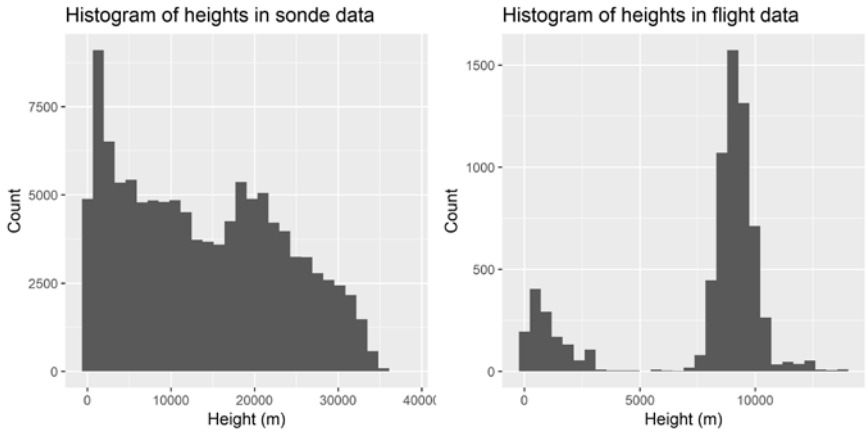


**FIGURE 6**
**HISTOGRAM OF ALTITUDES MEASURED IN THE NKX RADIOSONDE (LEFT) AND FLIGHTS WITHIN A 12 KM RADIUS OF THE NKX STATION**

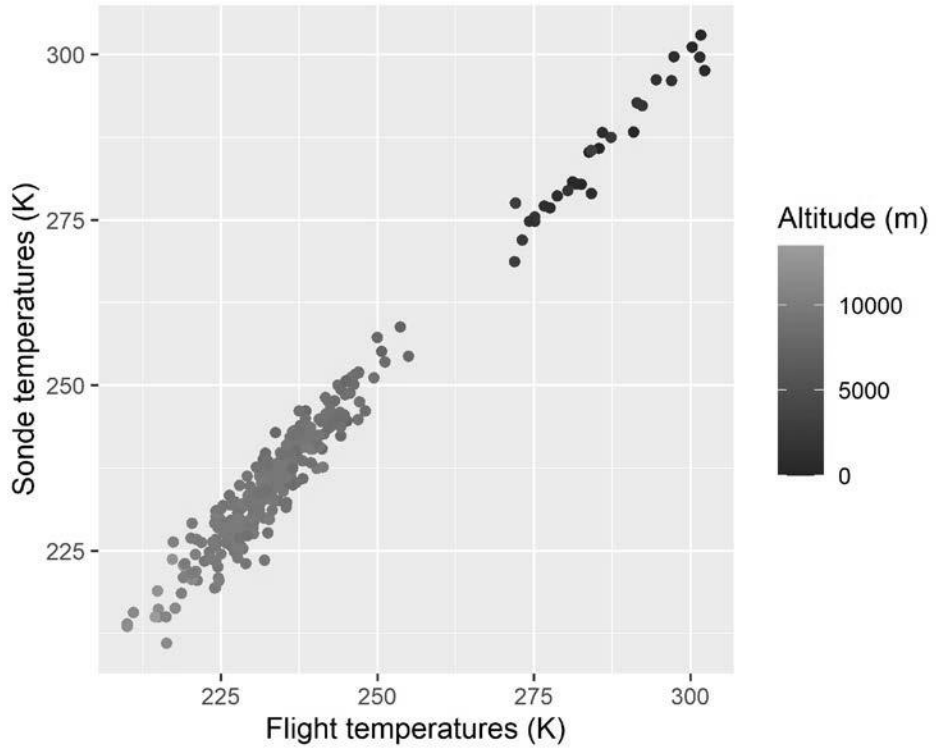


**FIGURE 7**
**SCATTERPLOT COMPARING TEMPERATURE MEASUREMENTS REPORTED BY ACARS (X-AXIS) AND THE RADIOSONDE AT NKX (Y-AXIS). MEASUREMENTS WERE ALIGNED BY THE HOUR AND BINNED INTO 50-METER INTERVALS. THE COLOR OF EACH POINT REPRESENTS THE ALTITUDE AT WHICH TEMPERATURES FROM BOTH DATA SOURCES WERE MEASURED**

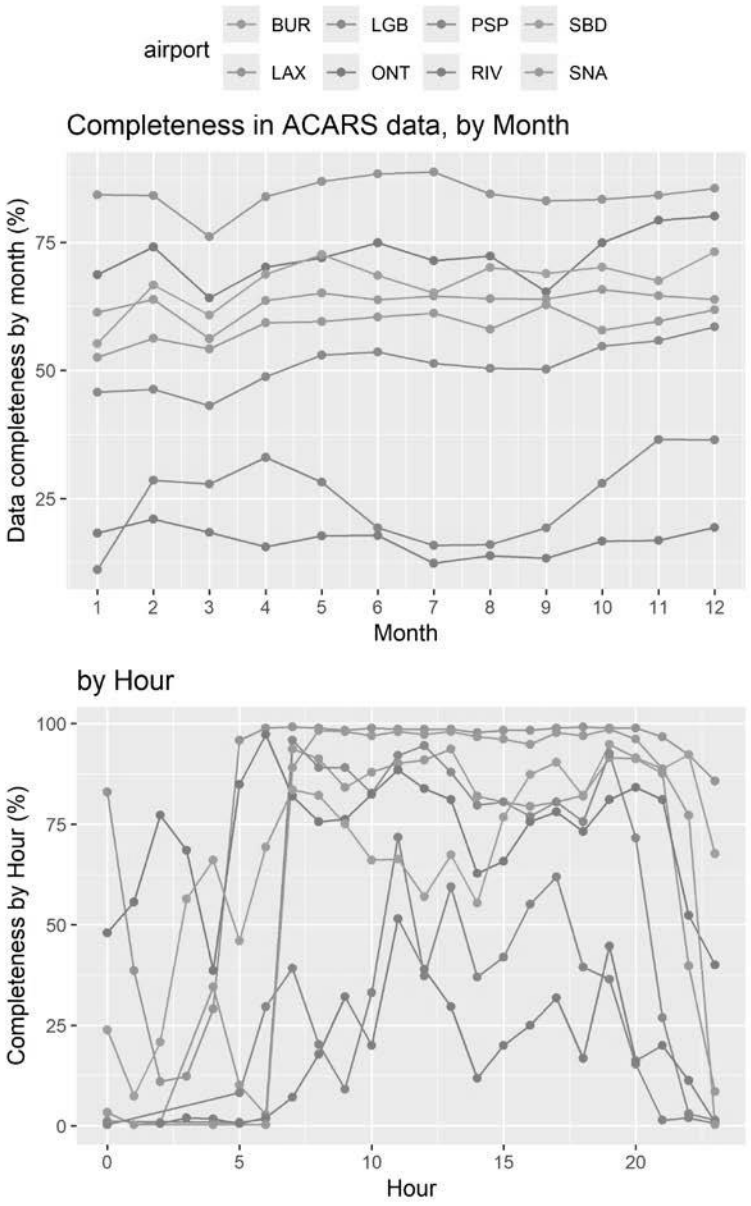


**FIGURE 8**
**PERCENTAGE OF DATA COMPLETENESS IN OBSERVED ACARS DATA BY AIRPORT, MONTH (TOP) AND HOUR (BOTTOM). PERCENTAGES WERE CALCULATED BY THE NUMBER OF OBSERVED DATA POINTS BY THE EXPECTED NUMBER FOR A GIVEN MONTH OR HOUR**

As shown in Figure 7, there is a high correlation between the radiosonde and flight datasets, indicating that both sources provide consistent atmospheric measurements within their respective ranges. This alignment suggests that despite differences in collection methods, the two datasets capture similar environmental conditions when compared at overlapping altitudes.

The observed gap in the data likely corresponds to the previously noted absence of lower-altitude flight observations around Miramar. As seen in earlier visualizations, this altitude range is underrepresented in aircraft data. Furthermore, a correlated relationship between radiosonde and flight data has also been documented in previous studies involving ACARS data (Zhang et al. 2022).

As seen on Figure 6, height profiles between radiosonde and flight data show significant variation. Flight data exhibits a bimodal distribution, with most observations concentrated around 10 kilometers—consistent with typical commercial flight altitudes. In contrast, radiosonde data is predominantly recorded at lower altitudes, reflecting its different sampling method and operational constraints. Radiosonde data has a much higher maximum altitude, recording data well above 30 km. On the other hand, flight data peak at a little over 10 km.

Compared to the modeled data described above, observed annual values estimated by ACARS are somewhat comparable to modeled results, but the data have notable limitations. Flight patterns are consistent and experience hourly variation. Hourly patterns are shown in Figure 8, where the bottom figure illustrates a large drop in data completeness after 10 pm, reflecting a large drop in flights. For example, some airports in the Basin, such as SNA (pink line, Figure 8) prohibit commercial departures and landings between 10 pm and 7 am and 11 pm and 7 am, respectively. Other airports see a similar drop in evening hours due to typical air traffic patterns.

The monthly results on show a large disparity in data completeness across each airport, reflecting the differing levels of air traffic handled at each site. While busy airports, such as LAX, have consistently high levels of data completeness, data from smaller regional or military airports, such as RIV and PSP are sparse.

# COMPARISON OF PBL HEIGHTS AND DISCUSSION

Figure 9 presents the monthly average diurnal variation of PBL height from NARR, NAM, NARR WRF, ERA5, and ACARS for the five stations: ONT, RIV, LAX, SNA, and PSP. The PSP station is included to evaluate PBL height in the Coachella Valley, which has different climate and land use characteristics from the South Coast Air Basin. AERMET derived PBL height from the inland stations ONT and RIV are also included.

Modeled PBL heights at each station were obtained by interpolating the nearest model predictions to the station locations using inverse distance weighting. Based on Figure 9, the following is observed:

- NARR data show high PBL peak values and elevated PBL levels during nighttime.
- NAM data shows low PBL height at ONT, LAX and PSP stations. The coarse spatial resolution of these datasets likely limits their ability to capture spatial variabilities in topography and surface features that influence PBL height development in the Basin.

- The PBL heights from ERA5 and NARR WRF show reasonable agreement with AERMET in their diurnal variation on ONT and RIV stations. However, ERA5 as well as NARR display much higher PBL height than other datasets at the PSP station.
- ACARS data fails to capture daily patterns shown by models, even at airports with seemingly sufficient data, such as LAX. While there are a large number of overall observations at some airports, splitting the data into individual hours and altitude intervals results in few observations at a given altitude and hour; at LAX, the number of observations at a given hour and altitude group ranges from one to five at altitudes above 500 meters. The scarcity of valid data poses uncertainties to use ACARS for those hours or even at certain airports. A consequence of a lack of data around RIV and PSP is that the distribution of altitudes is highly skewed, with higher altitudes (> 1500 m) overrepresented in RIV and lower altitudes (< 1000 m) overrepresented in PSP. As a result, PLBH estimates in PSP are especially low and those in RIV, while not entirely dissimilar from model estimates, appear inconsistent month-to-month, likely due to a lack of data. As shown on Figure 9, PBL heights estimated with ACARS data, while similar in magnitude to model estimates when summarized, do not exhibit the same hour-by-hour patterns expected of PBLH estimates.

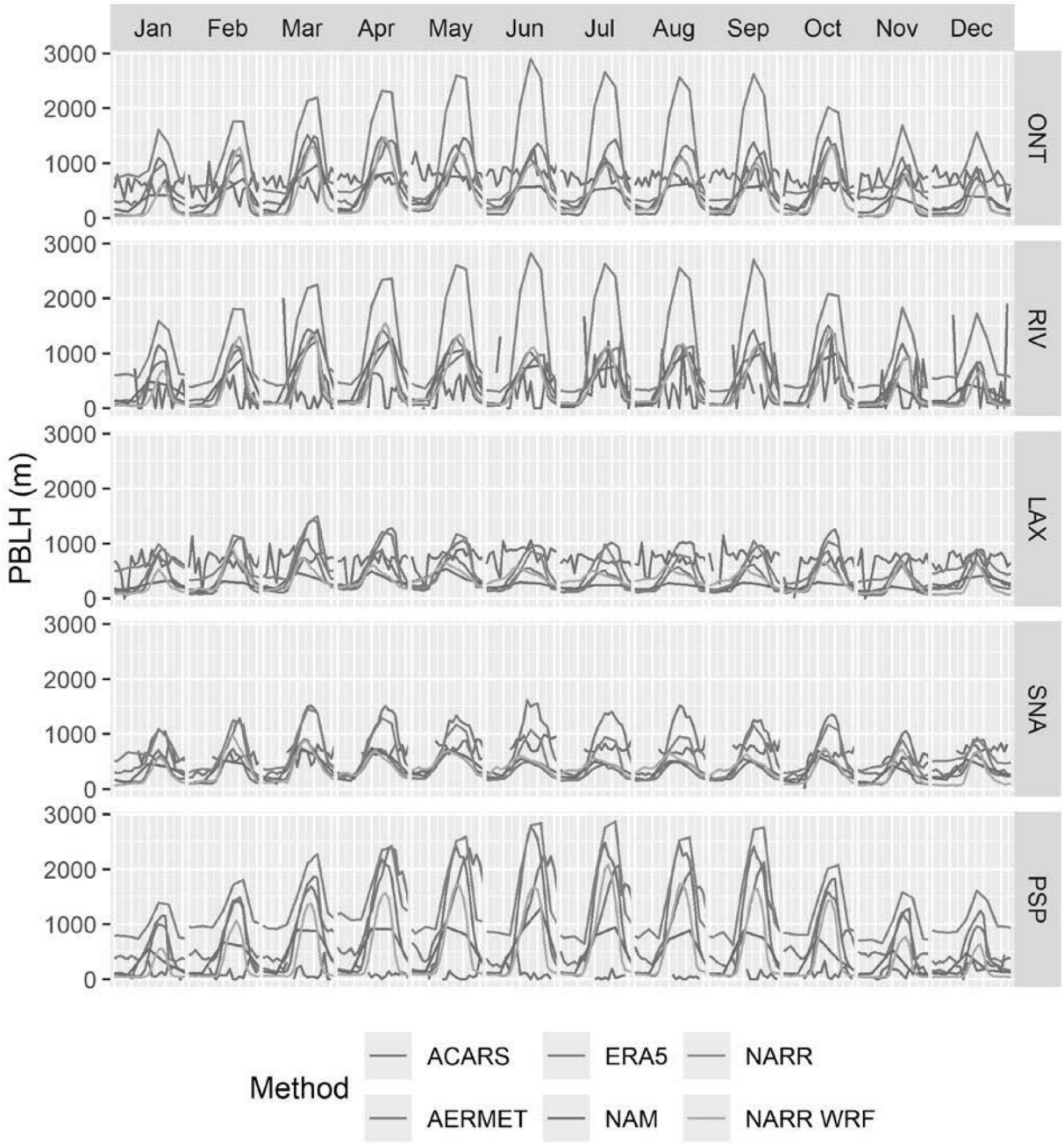


**FIGURE 9**

**DIURNAL VARIATION OF PBL HEIGHTS AVERAGED OVER EACH MONTH AT ONT, RIV, LAX, SNA, AND PSP. PBL HEIGHTS ARE ESTIMATED WITH NARR, NAM, NARR WRF, ERA5, AERMET, AND ACARS DATA**

Table 3 presents the PBL heights for selected airports based on various datasets. The hourly PBL heights were averaged over a year to create an annual average daily diurnal variation, and the maximum values from the average 24-hour period are presented here.

**TABLE 3**
**PBL HEIGHT VALUES FROM VARIOUS DATA SOURCES**

| | Airport | NARR WRF (m) | NARR (m) | NAM (m) | ERA5 (m) | AERMET (m) | ACARS (m) |
|---|---|---|---|---|---|---|---|
| LAX | Los Angeles International | 577 | 1,015 | 341 | 727 | N/A | 723 |
| ONT | Ontario International | 1,041 | 2,202 | 608 | 1,222 | 1,220 | 686 |
| SNA | John Wayne | 654 | 1,113 | 571 | 618 | N/A | 734 |
| LGB | Long Beach | 740 | 1,149 | 666 | 703 | N/A | 820 |
| BUR | Hollywood Burbank | 908 | 1,992 | 608 | 1,096 | N/A | 666 |
| SBD | San Bernardino International | 1,265 | 2,152 | 539 | 1,382 | N/A | 639 |
| PSP | Palm Springs international | 1,353 | 2,207 | 748 | 1,878 | N/A | 196 |
| RIV | March Air Force Reserve Base | 1,146 | 2,242 | 858 | 1,216 | 1,044 | 900 |

NARR and NAM analysis data, recorded at 3- and 6-hour intervals, respectively, could miss the daily maximum PBL and likely either overestimate or underestimate it due to their limited temporal resolution. In terms of spatial resolution, the NARR WRF simulation, with its 4x4 km grid, offers the highest level of detail, effectively capturing variations in land surface types and geographical characteristics which are essential for accurately simulating PBL height. The high resolution is desirable to capture location-specific PBL heights at multiple airport locations. The analysis intends to support aircraft emissions specified at 41 airports within the South Coast AQMD jurisdiction.[8]

In contrast, ERA5 data has a coarser resolution of approximately 25 km, providing limited spatial detail across the Basin. Zhang et al. (2020) reported that ERA5 tends to overestimate PBLH values over the U.S. by 18–41% relative to aircraft observations (Julaha et al., 2024). Additionally, Ou et al. (2020) found that ERA5 often peaks too early in the day. These findings suggest that some aspects of diurnal variability are not well captured in ERA5, likely due to its relatively coarse spatial and temporal resolution. Nonetheless, ERA5 shows reasonable estimates on an annual average and could be used in the absence of well calibrated high resolution meteorological modeling results or observations.

Figure 10 shows the map of the maximum PBL height from the diurnal variation averaged over a year, based on NARR WRF for the South Coast Air Basin and Coachella Valley. While some year-to-year

[8] Aircraft Emissions Inventory Report, South Coast AQMD (2025), https://www.aqmd.gov/docs/default-source/clean-air-plans/air-quality-management-plans/2022-air-quality-management-plan/emissions-inventory-methodology/aircraft-emissions-inventory-report.pdf?sfvrsn=965b6c7e_3

variation in PBL height is expected, preliminary NARR-WRF modeling for 2021 and 2023 shows that these variations are within 10% at all airport sites compared to the 2018 values. This suggests that interannual variability in PBL height using NARR-WRF is smaller than the differences observed between different datasets. Since the 2018 NARR-WRF dataset has undergone extensive evaluation for policy applications, this report bases its recommendations on the 2018 modeling results.

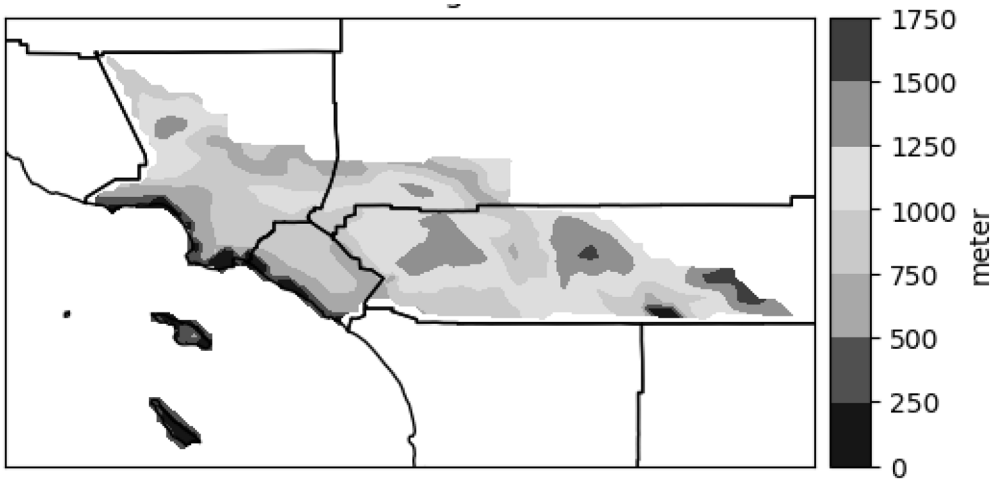


**FIGURE 10**
**MAXIMUM PBL HEIGHT FROM THE DIURNAL VARIATION AVERAGED OVER A YEAR FROM NARR WRF IN THE SOUTH COAST AIR BASIN AND THE COACHELLA VALLEY**

## SUMMARY AND CONCLUSION

This report evaluates several methods and datasets for estimating PBL height to be used in the development of the aircraft emissions inventory. Data sources include modeled products (ERA5, NARR, NAM, AERMET, and NARR-driven WRF) and ACARS aircraft data. Each method has advantages and limitations regarding spatial and temporal resolution, and coverage.

Results show that NARR data produce high PBL peaks and elevated nighttime values, while NAM underestimates PBL heights due to coarse spatial resolution and limited terrain representation. ERA5 and NARR-WRF generally align with AERMET observations at ONT and RIV, though ERA5 overestimate PBL heights at PSP. Observationally, ACARS data fail to reproduce diurnal PBL patterns attributed to poor data coverage, and while ACARS-derived PBL heights are comparable in magnitude to model values, their temporal patterns are unreliable for characterizing boundary layer evolution.

Overall, it is concluded that the maximum PBL height of an average day derived from NARR WRF data is the most appropriate to use as input for estimating aircraft emissions for the State Implementation Plan

(SIP) for the South Coast Air Basin and Coachella Valley. This is based on the capacity of the modeling system to resolve spatial and temporal variations at diverse airport locations reasonably well.

Moving forward, AQMD staff will continue improving the understanding of PBL dynamics and height through both model-based and observational data analysis. Collaborating with experts from academia and research groups will help refine PBL height estimates from both measurements and model predictions.

# REFERENCES


NOAA/Earth System Research Laboratory (ESRL). "Aircraft Meteorological Data Reports (AMDAR) and Aircraft Communications Addressing and Reporting System (ACARS) Data. Version 1.0." National Center For Atmospheric Research (NCAR), 2011, p. 5418. *DOI.org (Datacite)*, https://doi.org/10.26023/5FSS-TF0N-V906

Australian Government Bureau of Meteorology. (2012). *Ceilometer and visibility meters*. Retrieved from http://www.bom.gov.au/aviation/data/education/ceilometer-visibility.pdf

Caicedo, V., Rappenglück, B., Lefer, B., Morris, G., Toledo, D., & Delgado, R. (2017). Comparison of aerosol lidar retrieval methods for boundary layer height detection using ceilometer aerosol backscatter data. *Atmospheric Measurement Techniques*, *10*, 1609–1622.

Dai, C., et al. "Determining Boundary-Layer Height from Aircraft Measurements." *Boundary-Layer Meteorology*, vol. 152, no. 3, Sep. 2014, pp. 277–302.

English, Jason M., et al. "Creating a Convenient PBL Height Dataset Using Aircraft Data." [Boulder, CO], 2024, 2024 CIRES Rendezvous.

Hong, S.-Y., Noh, Y., & Dudhia, J. (2006). A new vertical diffusion package with an explicit treatment of entrainment processes. *Monthly Weather Review*, *134*, 2318–2341.

Julaha, K., Ždímal, V., Holubová Šmejkalová, A., Komínková, K., & Zíková, N. (2024). Boundary layer and mixing layer height: Models vs. ground-based measurements intercomparison. *Atmospheric Research*, *107897*.

Kalmus, P., Ao, C. O., Wang, K.-N., Manzi, M. P., & Teixeira, J. (2022). A high-resolution planetary boundary layer height seasonal climatology from GNSS radio occultations. *Remote Sensing of Environment*, *276*, 113037.

Roldán-Henao, N., Yorks, J. E., Su, T., Selmer, P. A., & Li, Z. (2024). Statistically resolved planetary boundary layer height diurnal variability using spaceborne lidar data. *Remote Sensing*, *16*(17), 3252.

Ou, T., Chen, D., Chen, X., Lin, C., Yang, K., Lai, H.-W., & Zhang, F. (2020). Simulation of summer precipitation diurnal cycles over the Tibetan Plateau at the gray-zone grid spacing for cumulus parameterization. *Climate Dynamics*, *54*, 3525–3539.

Seibert, P. (2000). Review and intercomparison of operational methods for the determination of the mixing height. *Atmospheric Environment*, *34*(7), 1001–1027.

Seidel, D. J., Ao, C. O., & Li, K. (2010). Estimating climatological planetary boundary layer heights from radiosonde observations: Comparison of methods and uncertainty analysis. *Journal of Geophysical Research: Atmospheres*, *115*, D16113.

Wagner, T. J., & Kleiss, J. M. (2016). Error characteristics of ceilometer-based observations of cloud amount. *Journal of Atmospheric and Oceanic Technology*, *33*, 1557–1567.

Zhang, D., Comstock, J., & Morris, V. (2022). Comparison of planetary boundary layer height from ceilometer with ARM radiosonde data. *Atmospheric Measurement Techniques*, *15*, 4735–4749.

Zhang, Y., Sun, K., Gao, Z., Pan, Z., Shook, M. A., & Li, D. (2020). Diurnal climatology of planetary boundary layer height over the contiguous United States derived from AMDAR and reanalysis data. *Journal of Geophysical Research: Atmospheres*, *125*(20).